Chemical Physics 370 (2010) 143–150

Contents lists available at ScienceDirect

Chemical Physics

journal homepage: www.elsevier.com/locate/chemphys

Quantum interferences and their classical limit in laser driven coherent control scenarios

Ignacio Franco [*,1], Michael Spanner [2], Paul Brumer

Chemical Physics Theory Group, Department of Chemistry, Center for Quantum Information and Quantum Control, University of Toronto, Toronto, ON, Canada M5S 3H6

ARTICLE INFO

Article history:
Received 24 September 2009
In final form 21 February 2010
Available online 25 February 2010

Keywords:
Coherent control
Quantum-classical correspondence
Quantum interference
Heisenberg dynamics

ABSTRACT

The analogy between Young's double-slit experiment with matter and laser driven coherent control schemes is investigated, and shown to be limited. To do so, a general decomposition of observables in the Heisenberg picture into direct terms and interference contributions is introduced, and formal quantum-classical correspondence arguments in the Heisenberg picture are employed to define classical analogs of quantum interference terms. While the classical interference contributions in the double-slit experiment are shown to be zero, they can be nonzero in laser driven coherent control schemes and lead to laser control in the classical limit. This classical limit is interpreted in terms of nonlinear response theory arguments.

© 2010 Elsevier B.V. All rights reserved.

1. Introduction

Identifying physical phenomena as quantum, as distinct from classical, has become of increasing interest due to modern developments in "quantum technologies", such as quantum information and computation, and quantum control [1,2]. Significantly, a variety of new results are emerging which enlighten as to what constitutes an inherently quantum feature. For example, several attributes often regarded as quantum in nature, such as the no-cloning theorem, the Born rule for probabilities and a Hilbert space structure for the dynamics, have been found to be features of classical mechanics as well [3–6].

Here we focus upon the role of quantum effects in the laser driven coherent control of atomic and molecular processes. Many of these processes have long been understood in terms of quantum interference effects exactly analogous to the ones in the double-slit experiment with matter. That is, the current view on coherent control phenomena is that the property that makes possible the active control of molecular dynamics is quantum interference, which arises from the fact that the behavior of material particles at molecular scales can be described in terms of waves [2,7–9]. The tool that permits practical exploitation of quantum interference for control of molecular dynamics is the laser, as it imparts a quantum phase on the system. Hence, by varying the laser phases one can vary the magnitude and sign of quantum interference contributions.

In this paper we examine the accuracy and generality of this analogy, with the goal of understanding whether laser driven coherent control is an explicitly quantum phenomenon or whether the same physical process is manifest classically as well. We do so using a framework, developed below, based upon the Heisenberg representation in quantum mechanics, an approach particularly well suited to examine the analogy between quantum mechanical and classical processes because it deals with dynamical variables directly instead of superposition states and probability amplitudes [10–12].

The question posed herein is somewhat subtle and requires clarification. Specifically, our focus is on whether various coherent control scenarios *qualitatively* require a quantum description, or whether they can *qualitatively* be described by classical mechanics. If the former is the case, then we will call the phenomenon inherently quantal in nature. This is in contrast to the circumstance where classical mechanics provides a qualitative description but fails to *quantitatively* describe observed results. For example, within this definition, tunnelling is a quantum process, but light absorption by molecules is not [13,14].

In addition to shedding light on the nature of laser control, the question posed is also of relevance practically. Specifically, if a phenomenon is indeed describable classically, then it is sensible to *consider* modelling the process in the classical limit using classical dynamics. This is not the case if it is a pure quantum phenomenon. Nonetheless, there is no implication that if a process can indeed be defined classically that a classical computation will provide an ade-

* Corresponding author.
E-mail address: ifranco@chem.northwestern.edu (I. Franco).
[1] Present address: Department of Chemistry, Northwestern University, Evanston, IL 60208-3113, United States.
[2] Present address: Steacie Institute for Molecular Sciences, National Research Council of Canada, Ottawa, ON, Canada K1A 0R6.

0301-0104/$ - see front matter © 2010 Elsevier B.V. All rights reserved.
doi:10.1016/j.chemphys.2010.02.016

quate quantitative result. Further, the resulting classical analogues, if they exist, offer alternative perspectives on well established coherent control schemes. Lastly, decoherence effects on laser control could be analyzed from a completely classical perspective [15] and may well offer insight into novel ways to combat it.

This problem may be regarded as ill-posed since, after all, nature is quantum and even the stability of matter requires a quantum description. Further, coherent control schemes often employ manifestly quantum phenomenon such as electronic transitions. Again, we do not question whether a *quantitative* account of laser control scenarios requires a quantum treatment. However, from a *qualitative* perspective the question still remains: is the wave character of matter *necessary* for the appearance of laser-induced interferences that can be used to control molecular dynamics?

This manuscript is organized as follows: In Section 2 we discuss the formal analogy between the double-slit experiment and laser driven coherent control schemes. For this we present a general decomposition of observables in the Heisenberg picture into direct terms and interference contributions, as well as a procedure to isolate the contributing terms. Then, in Section 3 we study such a decomposition in the classical limit and use it to define classical analogues of interference terms. With it, we extract interference contributions in a classical double-slit experiment and a classical laser control scenario. It is shown that the classical interference contributions in laser control can be nonzero and give origin to *classical* laser control. Our main results as well as a qualitative discussion of the nature of the "interference in the classical limit" are provided in Section 4.

2. Quantum interference

2.1. The double-slit experiment

The usual example used to explore quantum interference phenomena is Young's double-slit experiment with matter. In it, particles drawn, e.g., from a thermal distribution, are directed, at low intensity, at a barrier with two slits. A detector is placed at some distance behind the slits and the position of those particles that pass through the slits and arrive at the detection screen are recorded. In the classical case each particle can pass either through the upper or lower slit and there is no correlation between the two possibilities. The resulting probability distribution at the detection screen $P(y)$ is therefore the sum of the probability distributions $P_n(y)$ that would have been obtained if the experiment had been carried out with only slit $n = 1$ or slit $n = 2$, open,

$$P(y) = P_1(y) + P_2(y). \tag{1}$$

By contrast, in quantum mechanics there is an additional contributing term to $P(y)$, $P_{12}(y)$, to give

$$P(y) = P_1(y) + P_2(y) + P_{12}(y). \tag{2}$$

The term P_{12} arises from quantum interference effects, may be positive or negative, and is responsible for the appearance of fringes in the detection screen that cannot be accounted for through classical considerations.

Several compelling accounts of the double-slit experiment exist (see, for example, Refs. [16–19]). Below, we choose to describe it by considering the actual dynamics of the underlying scattering process in the Heisenberg picture. As will become evident, this perspective is particularly suitable to draw a parallel with coherent control phenomena and to study quantum interferences in the classical limit.

Suppose then that the particles to be diffracted are initially prepared in some state $|\phi_0\rangle$. For times $t < 0$ we imagine that the barrier has no slits and that at time $t = 0$ two slits are opened. The system is described by the Hamiltonian

$$\widehat{H}(t) = \widehat{H}_0 + \widehat{V}(t), \tag{3}$$

where $\widehat{H}_0$ is the Hamiltonian of the system plus barrier and

$$\widehat{V}(t) = \widehat{V}_1(t) + \widehat{V}_2(t) \tag{4}$$

describes the opening of the two slits, where $\widehat{V}_n$ describes opening slit n. Under the influence of $\widehat{H}(t)$ the system evolves into a superposition state

$$|\Psi(t)\rangle = \widehat{U}(t)|\phi_0\rangle, \tag{5}$$

determined by the evolution operator $\widehat{U}(t)$. Any interference effects that may arise during the experiment are completely characterized by $\widehat{U}(t)$ and by the initial state.

At this point it is convenient to express the evolution operator as

$$\widehat{U}(t) = \widehat{U}_0(t)\widehat{U}_{\rm I}(t), \tag{6}$$

where $\widehat{U}_0(t) = \exp(-i\widehat{H}_0 t/\hbar)$ characterizes the slit-free evolution of the system while $\widehat{U}_{\rm I}(t)$ quantifies the influence of the slits on the dynamics. Since $\widehat{U}(t)$ satisfies the Schrödinger equation $\left[i\hbar \frac{\rm d}{{\rm d}t}\widehat{U}(t) = \widehat{H}(t)\widehat{U}(t)\right]$, the dynamics of $\widehat{U}_{\rm I}$ is governed by

$$i\hbar\frac{\rm d}{{\rm d}t}\widehat{U}_{\rm I}(t) = \widehat{V}^{\rm I}(t)\widehat{U}_{\rm I}(t), \tag{7}$$

where

$$\widehat{V}^{\rm I}(t) = \widehat{U}_0^\dagger\widehat{V}(t)\widehat{U}_0 = \widehat{U}_0^\dagger\widehat{V}_1(t)U_0 + \widehat{U}_0^\dagger V_2(t)U_0 \equiv \widehat{V}_1^{\rm I}(t) + \widehat{V}_2^{\rm I}(t) \tag{8}$$

is the slit-opening component of the Hamiltonian in Interaction picture. Eq. (7) can be solved iteratively, yielding the well-known series [20]

$$\widehat{U}_{\rm I}(t) = \sum_{m=0}^{\infty}\widehat{U}_{\rm I}^{(m)}(t), \tag{9}$$

where $\widehat{U}_{\rm I}^{(0)}(t) = \hat{1}$ is a zeroth-order term and where

$$\widehat{U}_{\rm I}^{(m)}(t) = -\frac{i}{\hbar}\int_0^t {\rm d}t'\widehat{V}^{\rm I}(t')\widehat{U}_{\rm I}^{(m-1)}(t') \quad (m > 0) \tag{10}$$

describes the mth order contribution to $\widehat{U}_{\rm I}$, induced by $\widehat{V}(t)$.

The above equations suggest an exact partition of the evolution operator that exposes the interference phenomenon. Specifically, the evolution operator can be written as

$$\widehat{U}(t) = \widehat{U}_0(t) + \widehat{U}_1(t) + \widehat{U}_2(t) + \widehat{U}_{12}(t), \tag{11}$$

where $\widehat{U}_0(t)$ is the slit-free evolution operator, the term

$$\begin{aligned}&\widehat{U}_n(t) = \widehat{U}_0(t)\sum_{m=1}^{\infty}\widehat{U}_{{\rm I},n}^{(m)}(t) \quad (n = 1, 2)\\ &\text{with} \quad \widehat{U}_{{\rm I},n}^{(m)} = -\frac{i}{\hbar}\int_0^t {\rm d}t'\widehat{V}_n^{\rm I}(t')\widehat{U}_{{\rm I},n}^{(m-1)}(t') \quad (m > 0),\end{aligned} \tag{12}$$

is the additional contribution that would have been obtained if only slit n was open (i.e. if $\widehat{V}(t) = \widehat{V}_n(t)$), while

$$\widehat{U}_{12}(t) = \widehat{U}(t) - (\widehat{U}_0(t) + \widehat{U}_1(t) + \widehat{U}_2(t)) \tag{13}$$

represents all contributions to the evolution operator that explicitly depend on the existence of *both* $\widehat{V}_1$ and $\widehat{V}_2$. When $\widehat{U}(t)$ is applied to the initial state it produces a superposition state of the form

$$\begin{aligned}|\Psi(t)\rangle &= (\widehat{U}_0(t) + \widehat{U}_1(t) + \widehat{U}_2(t) + \widehat{U}_{12}(t))|\phi_0\rangle\\ &= |\psi_0(t)\rangle + |\psi_1(t)\rangle + |\psi_2(t)\rangle + |\psi_{12}(t)\rangle.\end{aligned} \tag{14}$$

Here $|\psi_0(t)\rangle$ represents that part of the wavefunction that gets reflected by the barrier, $|\psi_n(t)\rangle$ describes the part that passes through slit n, and $|\psi_{12}(t)\rangle$ contains any additional contributions that involve the two slits.

In light of Eq. (11) it follows that the evolution of any observable $\widehat{O}^{\rm H}(t) = \widehat{U}^{\dagger}(t)\widehat{O}\widehat{U}(t)$ in the Heisenberg picture admits the decomposition

$$\widehat{O}^{\rm H}(t) = \widehat{O}_0^{\rm H}(t) + \widehat{O}_1^{\rm H}(t) + \widehat{O}_2^{\rm H}(t) + \widehat{O}_{12}^{\rm H}(t). \tag{15}$$

Here

$$\widehat{O}_0^{\rm H}(t) = \widehat{U}_0^{\dagger}\widehat{O}\widehat{U}_0 \tag{16}$$

describes the dynamics of the observable in the absence of slits, the term

$$\widehat{O}_n^{\rm H}(t) = \widehat{U}_0^{\dagger}\widehat{O}\widehat{U}_n + \widehat{U}_n^{\dagger}\widehat{O}\widehat{U}_0 + \widehat{U}_n^{\dagger}\widehat{O}\widehat{U}_n \tag{17}$$

quantifies the additional contribution to the observable if only slit n is open, while

$$\begin{aligned}\widehat{O}_{12}^{\rm H}(t) = {} & \widehat{U}_1^{\dagger}\widehat{O}\widehat{U}_2 + \widehat{U}_2^{\dagger}\widehat{O}\widehat{U}_1 + (\widehat{U}_0^{\dagger} + \widehat{U}_1^{\dagger} + \widehat{U}_2^{\dagger})\widehat{O}\widehat{U}_{12} \\ & + \widehat{U}_{12}^{\dagger}\widehat{O}(\widehat{U}_0 + \widehat{U}_1 + \widehat{U}_2) + \widehat{U}_{12}^{\dagger}\widehat{O}\widehat{U}_{12}\end{aligned} \tag{18}$$

describes the interference contributions.

The structure of Eq. (15) is characteristic of situations that involve interference. It contains two direct terms $\widehat{O}_n^{\rm H}$ and an interference contribution $\widehat{O}_{12}^{\rm H}$. Note that Eq. (2) is a particular case of Eq. (15) obtained by demanding that the relevant operator measures the position y of the particles on a detector located at $x = L > 0$, i.e. $\widehat{O} = \widehat{P} = |x = L\rangle|y\rangle\langle y|\langle x = L|$. If the particles are initially prepared to the left of the barrier $x < 0$ then $\langle\widehat{P}_0^{\rm H}\rangle = 0$ as particles cannot cross the barrier when the two slits are closed. Hence, from Eq. (15) it follows that

$$P(y,t) = P_1(y,t) + P_2(y,t) + P_{12}(y,t), \tag{19}$$

where $P_n(y,t) = \langle\widehat{P}_n^{\rm H}\rangle$ is the probability that the particle crossed the barrier through slit n and arrived at the screen at position y and time t, while $P_{12}(y,t)$ quantifies the interference between the two possibilities. The angle brackets here and below denote an average over the initial wavefunction. In the actual experiment only an integrated signal is recorded and Eq. (2) is recovered by integrating Eq. (19) over time.

An important aspect of the partitioning in Eq. (15) is that by using it one can design an experimental procedure to isolate interference contributions. In a first experiment, the two slits are closed and the observable of interest is measured, giving $\langle\widehat{O}_0^{\rm H}(t)\rangle$. Subsequently, two additional experiments are performed in which only slit n is opened and $\langle\widehat{O}^{\rm H}(t)\rangle$ measured, giving $\langle\widehat{O}_n^{\rm H}(t)\rangle = \langle\widehat{O}^{\rm H}(t)\rangle - \langle\widehat{O}_0^{\rm H}(t)\rangle$. In a final experiment the dynamics of the observable is followed with both slits open. The contributions due to interference are then given by $\langle\widehat{O}_{12}^{\rm H}(t)\rangle = \langle\widehat{O}^{\rm H}(t)\rangle - (\langle\widehat{O}_0^{\rm H}(t)\rangle + \langle\widehat{O}_1^{\rm H}(t)\rangle + \langle\widehat{O}_2^{\rm H}(t)\rangle)$.

2.2. Laser control

The above analysis is general and can be used to study interferences induced by any perturbing potential $\widehat{V}(t)$ with two or more components. Through the set of experiments described above, or slight variations of them, correlations between competing dynamical processes embedded within $\widehat{V}(t)$ can be quantified. Consider then these ideas applied to laser control scenarios in which $\widehat{V}(t)$, instead of opening slits on a barrier, describes the interaction of the system with components of a laser field. The procedure is completely parallel to the one presented above. Nevertheless, we repeat aspects of it in order to stress the analogy between the two physical situations.

2.2.1. N vs. M control

Consider then a molecular system with Hamiltonian $\widehat{H}_0$ interacting with a radiation field $\boldsymbol{E}(t)$ in the dipole approximation. The total Hamiltonian of the system is $\widehat{H}(t) = \widehat{H}_0 + \widehat{V}(t)$, where

$$\widehat{V}(t) = -\hat{\boldsymbol{\mu}}\cdot\boldsymbol{E}(t) \tag{20}$$

is the radiation-matter interaction term and $\hat{\boldsymbol{\mu}}$ is the system's dipole operator. For simplicity we focus on the case where each competing dynamical process is determined by a different frequency component of the radiation field. This physical situation encompasses, for example, the 1 vs. 2 and the 1 vs. 3 coherent control schemes in which $\omega + 2\omega$ and $\omega + 3\omega$ fields are used to photoexcite the system, respectively. These control scenarios are two important examples of the general class of N vs. M control schemes [2].

When a two-color laser $\boldsymbol{E}(t) = \boldsymbol{\epsilon}_1 E_1(t) + \boldsymbol{\epsilon}_2 E_2(t)$ is incident on the system the radiation-matter interaction term can be written as $\widehat{V}(t) = \widehat{V}_1(t) + \widehat{V}_2(t)$, where

$$\widehat{V}_n(t) = -\hat{\boldsymbol{\mu}}\cdot\boldsymbol{\epsilon}_n E_n(t) \quad (n = 1,2) \tag{21}$$

describes the interaction of the system with the nth component of the field. As before, the evolution operator admits the decomposition

$$\widehat{U}(t) = \widehat{U}_0(t) + \widehat{U}_1(t) + \widehat{U}_2(t) + \widehat{U}_{12}(t), \tag{22}$$

where $\widehat{U}_0 = \exp(-i\widehat{H}_0 t/\hbar)$ is the field-free evolution operator, $\widehat{U}_n$ is the correction term that would have been obtained if the system evolved solely under $\widehat{V}_n(t)$, while $\widehat{U}_{12}$ represents contributions that appear when both colors are present. In analogy with Eq. (14), when $\widehat{U}(t)$ acts on the initial state it produces a superposition state of the form

$$\begin{aligned}|\Psi(t)\rangle &= (\widehat{U}_0(t) + \widehat{U}_1(t) + \widehat{U}_2(t) + \widehat{U}_{12}(t))|\phi_0\rangle \\ &= |\psi_0(t)\rangle + |\psi_1(t)\rangle + |\psi_2(t)\rangle + |\psi_{12}(t)\rangle.\end{aligned} \tag{23}$$

Here $|\psi_0(t)\rangle$ represents the field-free evolution of the system, $|\psi_n(t)\rangle$ the excitation produced by the nth component of the field, while $|\psi_{12}(t)\rangle$ contains any additional corrections that explicitly involve both $\widehat{V}_1$ and $\widehat{V}_2$.

As in the double-slit experiment, the Heisenberg dynamics of any observable $\widehat{O}$ admits the decomposition

$$\widehat{O}^{\rm H}(t) = \widehat{O}_0^{\rm H}(t) + \widehat{O}_1^{\rm H}(t) + \widehat{O}_2^{\rm H}(t) + \widehat{O}_{12}^{\rm H}(t). \tag{24}$$

Here $\widehat{O}_0^{\rm H}$ describes the field-free dynamics, the direct terms $\widehat{O}_n^{\rm H}$ quantify contributions that arise when only the nth color of the field is turned on, while $\widehat{O}_{12}^{\rm H}$ represents the interference contributions that are at the heart of laser control phenomena. Further, using Eq. (24) one can design a set of experiments to isolate the interference contributions. In a first experiment the system is allowed to evolve in the absence of lasers, giving $\langle\widehat{O}_0^{\rm H}(t)\rangle$. Then two additional experiments with either laser, $n = 1$ or 2, on are performed from which $\langle\widehat{O}_n^{\rm H}(t)\rangle$ can be extracted. Last, by subjecting the system to both laser fields and measuring $\langle\widehat{O}^{\rm H}(t)\rangle$ one has sufficient information to isolate the interference contributions.

2.2.2. Bichromatic control

The bichromatic control scenario [2,7] represents yet another class of control schemes, with formal equivalence to pump–dump schemes and to the 2 vs. 2 control scenario [2]. In this scenario the system is first prepared in a superposition of two Hamiltonian eigenstates. This initial superposition is subsequently photodissociated to a given energy in the continuum using a two-color laser field with frequency components ω_2 and ω_3. The frequencies of the dissociating pulse are selected such that $|\omega_3 - \omega_2|$ matches exactly the Bohr transition frequency between the states involved in the initial superposition.

Consider this scenario in the Heisenberg picture. For this we suppose that the preparation and dissociation stages occur at two different times, so that

$$\hat{U}(t,t_0)=\hat{U}_{\rm diss}(t,t_1)\hat{U}_{\rm prep}(t_1,t_0)\quad (t>t_1>t_0). \tag{25}$$

Here $\hat{U}_{\rm prep}(t_1,t_0)$ and $\hat{U}_{\rm diss}(t,t_1)$ are the evolution operators during preparation and dissociation, respectively. The initial superposition state is achieved by exciting the system between times t_0 and t_1 with a laser (field 1) resonantly coupling the two desired levels. The dynamics during the process is characterized by

$$\hat{U}_{\rm prep}(t_1,t_0)=\hat{U}_0(t_1,t_0)+\hat{U}_1(t_1,t_0), \tag{26}$$

where $\hat{U}_0(t_1,t_0)$ is the field-free evolution operator, while $\hat{U}_1(t_1,t_0)$ describes the excitation process induced by field 1. During dissociation (for times $t>t_1$) the evolution operator is given by

$$\hat{U}_{\rm diss}(t,t_1)=\hat{U}_0(t,t_1)+\hat{U}_2(t,t_1)+\hat{U}_3(t,t_1)+\hat{U}_{23}(t,t_1). \tag{27}$$

Here $\hat{U}_n(t,t_1)$ with n = 2 or 3 represents the influence of the nth dissociating field on the dynamics, while $\hat{U}_{23}(t,t_1)$ quantifies any additional corrections to the evolution that depend on the presence of both fields. Using this partitioning, one can decompose the Heisenberg evolution of any observable as:

$$\hat{O}^{\rm H}(t)=\hat{O}^{\rm H}_0(t)+\hat{O}^{\rm H}_1(t)+\hat{O}^{\rm H}_2(t)+\hat{O}^{\rm H}_3(t)+\hat{O}^{\rm H}_{12}(t)+\hat{O}^{\rm H}_{13}(t)+\hat{O}^{\rm H}_{23}(t)+\hat{O}^{\rm H}_{123}(t). \tag{28}$$

Here $\hat{O}^{\rm H}_0(t)$ is the field-free evolution, $\hat{O}^{\rm H}_n(t)$ with $n=1,2,3$ is the term that would have been obtained if only field n was turned on, $\hat{O}^{\rm H}_{nm}(t)$ represents the interferences between pairs of competing dynamical processes onset by pulses n and m $(n\neq m)$, while $\hat{O}^{\rm H}_{123}(t)$ is the interference contributions that depend on the three fields. As this scenario involves three fields, eight experiments are required to isolate all contributing terms to $\langle\hat{O}^{\rm H}(t)\rangle$.

3. Interferences in the classical limit

A crucial property of the partitions introduced in Section 2 is that each of the contributing terms entering into $\hat{O}^{\rm H}(t)$ has a well-defined classical $(\hbar=0)$ limit. In this section we exploit this property to define classical analogues of quantum interference terms. Central to this analysis is the quantum-classical correspondence principle in the Heisenberg picture. We thus begin by studying the classical limit of the Heisenberg dynamics [10,11], as it permits identifying the $\hbar=0$ limit of quantum observables in the Heisenberg picture with the phase-space flow of the corresponding classical observable.

3.1. Heisenberg dynamics in the classical limit

Consider an observable $\hat{O}$ in the Schrodinger picture with no explicit time dependence. The dynamics of $\hat{O}$ in the Heisenberg picture is governed by the Heisenberg equations of motion

$$\frac{\rm d}{{\rm d}t}\hat{O}^{\rm H}(t)=\frac{1}{i\hbar}[\hat{O}^{\rm H}(t),\hat{H}^{\rm H}(t)]. \tag{29}$$

The interest here is to study $\hat{O}^{\rm H}(t)$, and the above differential equation for operators, in the classical limit. For this it is convenient to represent $\hat{O}^{\rm H}(t)$ and Eq. (29) in the phase space of c-number position x and momentum p variables, and then take the classical $(\hbar=0)$ limit. A phase space picture of $\hat{O}^{\rm H}(t)$ can be obtained using the Wigner transform [21,22], defined as

$$O_{\rm W}(x,p)=\int {\rm d}v\ {\rm e}^{-{\rm i}pv/\hbar}\left\langle x+\frac{1}{2}v|\hat{O}|x-\frac{1}{2}v\right\rangle. \tag{30}$$

Through this transformation each quantum operator $\hat{O}$ is represented by a unique phase space function $O_{\rm W}(x,p)$ and, conversely, each symbol $O_{\rm W}(x,p)$ defines an operator in Hilbert space. Using Groenewold's identity [23] for the Wigner transform of a product of operators:

$$(\hat{A}\hat{B})_{\rm W}=A_{\rm W}(x,p)\exp\left[\frac{i\hbar}{2}\left(\frac{\overleftarrow{\partial}}{\partial x}\frac{\overrightarrow{\partial}}{\partial p}-\frac{\overleftarrow{\partial}}{\partial p}\frac{\overrightarrow{\partial}}{\partial x}\right)\right]B_{\rm W}(x,p), \tag{31}$$

where the arrows indicate the direction in which the derivatives act, Eq. (29) becomes

$$\frac{\rm d}{{\rm d}t}(\hat{O}^{\rm H})_{\rm W}=(\hat{O}^{\rm H})_{\rm W}\frac{2}{\hbar}\sin\left\{\frac{\hbar}{2}\left(\frac{\overleftarrow{\partial}}{\partial x}\frac{\overrightarrow{\partial}}{\partial p}-\frac{\overleftarrow{\partial}}{\partial p}\frac{\overrightarrow{\partial}}{\partial x}\right)\right\}(\hat{H}^{\rm H})_{\rm W}, \tag{32}$$

which provides a phase space description of the Heisenberg dynamics.

Eq. (32) has a well-defined classical $(\hbar=0)$ limit provided that $(\hat{O}^{\rm H})_{\rm W}$ and $(\hat{H}^{\rm H})_{\rm W}$ are semiclassically admissible [10]. That is, that one can express these functions in a series

$$(O^{\rm H})_{\rm W}(x,p,t)=O^{\rm c}(x,p,t)+\sum_{n=1}^{\infty}\frac{\hbar^n}{n!}o_n(x,p,t) \tag{33}$$

that is asymptotically regular at $\hbar=0$ for finite times. If this is the case, by letting $\hbar=0$ in Eq. (32) one recovers Hamilton's equations of motion

$$\frac{\rm d}{{\rm d}t}O^{\rm c}(x,p,t)=\{O^{\rm c}(x,p,t),H^{\rm c}(x,p,t)\}, \tag{34}$$

where $\{f,H^{\rm c}\}=\frac{\partial f}{\partial x}\frac{\partial H^{\rm c}}{\partial p}-\frac{\partial f}{\partial p}\frac{\partial H^{\rm c}}{\partial x}$ is the Poisson bracket and $O^{\rm c}(x,p,t)$ and $H^{\rm c}(x,p,t)$ are regarded as the classical counterparts of $\hat{O}^{\rm H}$ and $\hat{H}^{\rm H}$, respectively.

Now, for $(\hat{O}^{\rm H})_{\rm W}$ and $(\hat{H}^{\rm H})_{\rm W}$ to satisfy Eq. (33) only requires that $(\hat{x}^{\rm H})_{\rm W}$ and $(\hat{p}^{\rm H})_{\rm W}$ are semiclassically admissible. This property is an important consequence of Eq. (31) which shows that the product of two semiclassically admissible operators is also semiclassically admissible, and holds provided that $\hat{O}$ and $\hat{H}$ are expressible in terms of products of the position $\hat{x}$ and momentum $\hat{p}$ operators.

At the initial time common observables such as position, momentum, angular momentum and the Hamiltonian are semiclassically admissible. Further, the leading term in the $\hbar$-expansion coincides with the familiar quantities of classical mechanics. Hence, the main assumption in this quantum-classical correspondence principle is that semiclassical admissibility is stable under time evolution for the position and momentum operators. If this is the case, then one can identify the $\hbar=0$ limit of an observable in the Heisenberg picture with the phase-space flow of the corresponding classical observable. Recent work by Osborn [24] has established conditions for the stability of Eq. (33) under time evolution.

Note that this formal correspondence between quantum and classical observables does not apply to the density matrix by itself. The Wigner representation for pure state density matrices is singular [10] at $\hbar=0$ and hence it is not semiclassically admissible even at the initial time.

3.2. Classical partitions of observables

Insofar as the above correspondence rule holds, one can apply the analysis in Section 2 to study correlations between competing dynamical processes in classical systems. Consider, for example, the general partitioning of observables in Eq. (15):

$$\hat{O}^{\rm H}(t)=\hat{O}^{\rm H}_0(t)+\hat{O}_1{}^{\rm H}(t)+\hat{O}^{\rm H}_2(t)+\hat{O}^{\rm H}_{12}(t). \tag{15}$$

If $\hat{O}$ is semiclassically admissible and the four Hamiltonians determining the different contributions to the dynamics ($\hat{H}_0$, $\hat{H}_0+\hat{V}_1$, $\hat{H}_0+\hat{V}_2$ and $\hat{H}_0+\hat{V}_1+\hat{V}_2$) are also semiclassically admissible with nonzero classical counterpart then each term in the above equation has a well defined classical limit of the form

$$O^c(t) = O_0^c(t) + O_1^c(t) + O_2^c(t) + O_{12}^c(t), \quad (35)$$

where the different contributions to $O^c(t)$ are the classical counterparts of the corresponding terms in Eq. (15). Using the example of the double-slit experiment, O_0^c describes the classical flow of the observable in the absence of slits, O_n^c quantifies the additional contributions to the observable if only slit n is open, while O_{12}^c quantifies any classical correlations between the two possibilities. The latter term is the classical limit of the quantum interference contributions to the observable. By analogy with the quantum language we will refer to it as the classical interference term.

It is important to note that this connection between quantum and classical mechanics makes no reference to the initial state. In a *quantitative* comparison, quantum contributions arising from the dynamics of observables and from the quantum nature of the initial state need to be taken into account. However, from a *qualitative* perspective this aspect is immaterial; for if matter interference effects are *in principle* the origin of laser control then under completely classical conditions no laser control should be possible, i.e. $O_{12}^c(t)$ should be zero.

Hence, in this analysis classical averages are obtained by weighting $O^c(t)$ by an ensemble of classical initial conditions $\rho_c(x,p)$:

$$\langle O^c(t)\rangle_c = \mathrm{Tr}\{O^c(t)\rho_c(x,p)\}. \quad (36)$$

The classical interference contributions to the observable $\langle O_{12}^c(t)\rangle_c$ can be isolated and quantified by repeating the set of experiments described above for the quantum case but by using a classical initial distribution that evolves according to the classical equations of motion. We now consider two examples: the double-slit experiment and the 1 vs. 2 laser control scenario. If the analogy between these two physical situations is faithful, one would expect the interference contributions in both cases to be zero.

3.2.1. Example: the double-slit experiment

Fig. 1 shows the setup of the classical double-slit numerical experiment. The observable of interest is the distribution of particles at the detection screen $P^c(y)$. In this example, $P_0^c(y) = 0$ since the particles cannot cross the barrier when the two slits are closed.

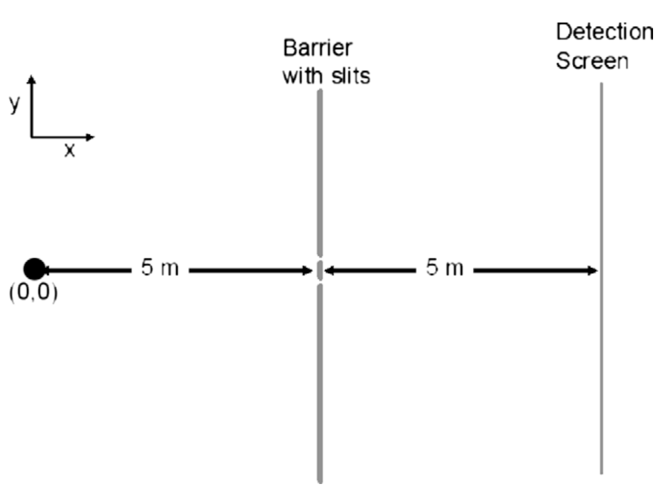

Fig. 1. Scheme of the double-slit experiment. Particles are directed at the barrier starting from a Gaussian distribution centered at the black dot in the figure $(x_0, y_0) = (0,0)$ with spatial width $\Delta x = \Delta y = 20\ \mu$m. The mean velocities of the initial state are $v_x^0 = 200\ \mathrm{m\,s^{-1}}$ and $v_y^0 = 0\ \mathrm{m\,s^{-1}}$ with a spread of $\Delta v_x^0 = \Delta v_y^0 = 7.5\ \mathrm{m\,s^{-1}}$. The barrier is 0.2 m in width. The slits are 0.15 m long and 0.35 m apart.

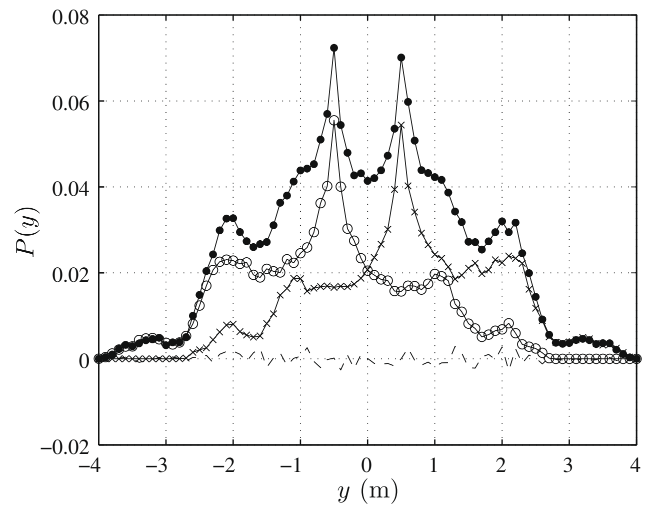

Fig. 2. Probability density distribution at the detection screen of the double-slit experiment schematically shown in Fig. 1 after launching 300,000 particles. The •'s correspond to the case in which the two slits are open. The ∘'s and ×'s to the one in which only the lower or upper slit is open, respectively. The broken line represents the classical interferences in the observable $P_{12}^c(y)$.

Fig. 2 shows the results for the remaining three experiments and the resulting classical interference terms in the observable $P_{12}^c(y)$ (broken line). We observe that within statistical errors the classical particles do not exhibit any kind of correlations between the two classical possibilities. That is, as expected, the probability density observed at the screen is merely the sum of the probabilities of particles going through each of the slits. The observed classical behavior is a consequence of the fact that classical particles do not have a wave character.

3.2.2. Example: 1 vs. 2 control

In this scenario a spatially symmetric system is driven with an $\omega + 2\omega$ field. In quantum mechanics the interference between the one-photon absorption induced by the 2ω-component and the two-photon absorption process induced by the ω-component results in phase-controllable transport. We now study this scenario from a completely classical perspective.

As a system we choose an ensemble of noninteracting particles of mass m and charge q initially confined in the one-dimensional

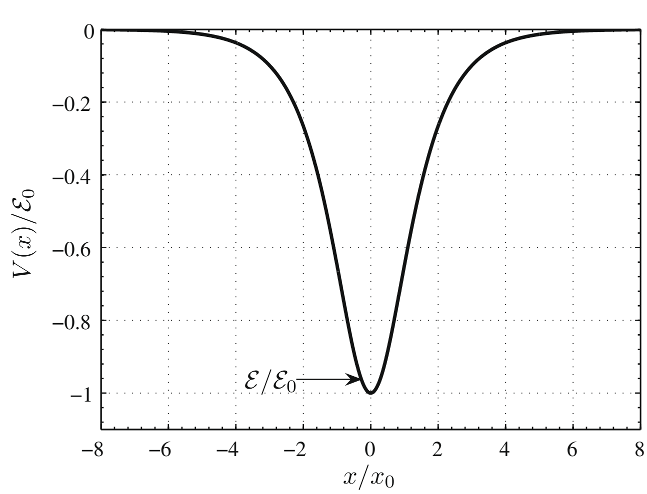

Fig. 3. Bounding potential $V(x) = -\mathscr{E}_0/\cosh(x)$ for the one-dimensional model system. The initial state is an ensemble of initial conditions with constant energy $\mathscr{E} = -0.95\mathscr{E}_0$. Here x_0 is some characteristic length.

potential schematically shown in Fig. 3. As an initial distribution we choose a microcanonical ensemble with energy $\mathscr{E} = -0.95\mathscr{E}_0$, where $-\mathscr{E}_0$ is the minimum of the potential. At time $t = 0$ the system is allowed to interact with an $\omega + 2\omega$ Gaussian laser pulse, so that the components $(n = 1, 2)$ of the radiation-matter interaction term are given by

$$V_n(t) = -qx\epsilon_{n\omega}\cos(n\omega t + \phi_{n\omega} + n\alpha)\exp\left[-\left(\frac{t - T_c}{T_w}\right)^2\right]. \tag{37}$$

The pulse has width $T_w = 100t_0$ and is centered at time $T_c = 3T_w$ where $t_0 = \sqrt{mx_0/\mathscr{E}_0}$ is a characteristic time and x_0 a characteristic length. We choose $\epsilon_\omega = 0.66\mathscr{E}_0/(qx_0)$, $\epsilon_{2\omega} = 0.33\mathscr{E}_0/(qx_0)$ and $\omega t_0 = 0.45$. Interest is in isolating effects that depend solely on

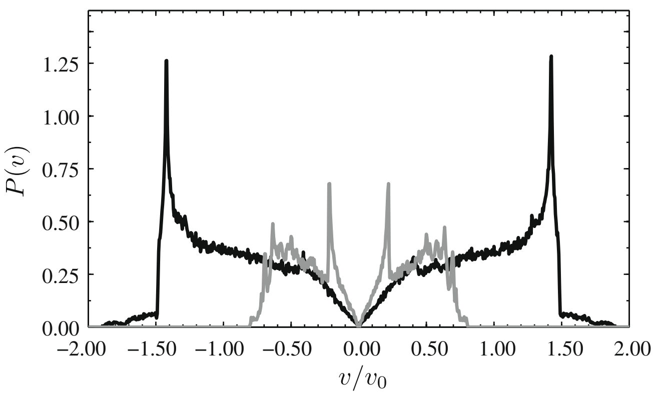

Fig. 4. Velocity probability density $P^c(v)$ for particles dissociated by the ω-component $P_1^c(v)$ (black line) and the 2ω component $P_2^c(v)$ (gray line) of the laser field. Here $v_0 = x_0/t_0$ is a characteristic velocity.

the relative phase $2\phi_\omega - \phi_{2\omega}$ between the two laser components, i.e., one of the control variables. Hence the calculations presented here are averaged over the carrier envelope phase $\alpha \in [0, 2\pi)$ of the laser field, done by randomly selecting an α for each member of the ensemble.

As an observable we choose the velocity distribution $P^c(v)$ of the photoejected particles after the laser field is turned off. Any rectification effects should manifest as anisotropy in $P^c(v)$. Using the decomposition in Eq. (35),

$$P^c(v) = P_0^c(v) + P_1^c(v) + P_2^c(v) + P_{12}^c(v), \tag{38}$$

where $P_0^c(v)$ is the field-free ensemble average of the observable, $P_n^c(v)$ the additional contributions induced by the $n\omega$-component of the field, and $P_{12}^c(v)$ the classical interferences. In this case, $P_0^c(v) = 0$ as no photodissociation can occur in the absence of the field. Fig. 4 shows the results of the experiment when only one of the field's components is used. The resulting probability density $P_n^c(v)$ exhibits a right/left symmetry and no net currents are generated. The situation is completely different when both the ω and the 2ω components are applied (Fig. 5). The $\omega + 2\omega$ field generates anisotropy in $P^c(v)$. Further, the degree and magnitude of the effect can be manipulated by varying the relative phase between the two frequency components of the beam. The resulting classical interference terms are shown in gray. In stark contrast to the double-slit experiment, the interference between the two laser-induced dynamical processes is nonzero and is the origin of the rectification effect. Moreover, $P_{12}^c(v)$ can take positive or negative values and is phase-controllable, just as its quantum counterpart.

Supplementary analyses and additional work on this control scenario are worth noting. Ref. [11] provides an analytical treatment of the 1 vs. 2 photon case for a quartic oscillator, and a detailed analysis of the classical limit. Ref. [25] shows how the laser-induced symmetry breaking effect can be accounted for in both

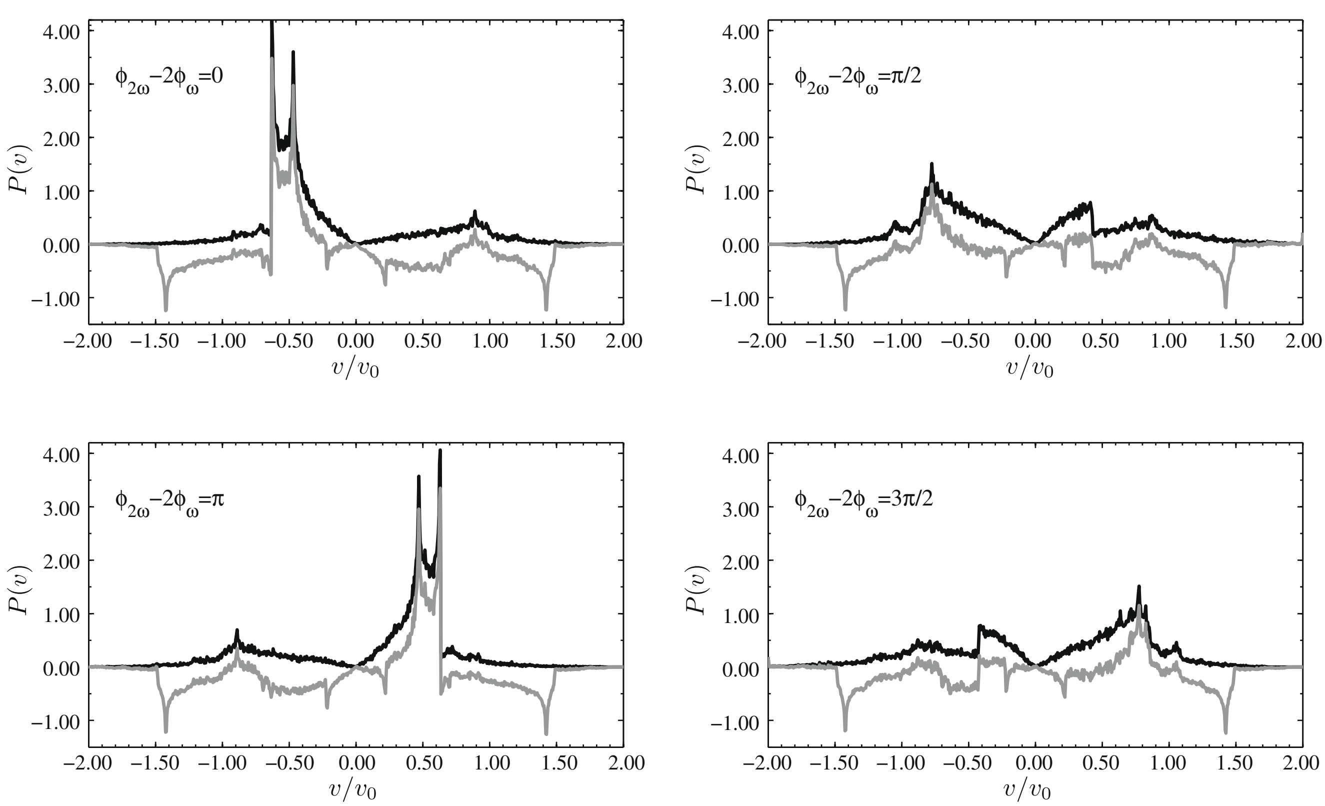

Fig. 5. Velocity probability density $P^c(v)$ for particles dissociated by an $\omega + 2\omega$ field (black lines) for different relative laser phases. The interference contributions $P_{12}^c(v)$ in each experiment are plotted in gray.

quantum and classical mechanics through a single symmetry analysis of the equations of motion. Recent further studies [26] propose and analyze a specific optical lattice realization of this control scenario, where the approach to the classical limit is expected to be observable experimentally.

4. Summary and discussion

Our discussion has focused on coherent control scenarios involving multiple laser-induced dynamical pathways. In doing so we have considered the analogy between the double-slit experiment and laser driven multiple-path control scenarios. In both cases the system is subject to two or more competing dynamical processes and the quantum evolution results in a superposition state with exactly analogous analytical structure [recall Eqs. (14) and (23)]. Further, the interference contributions that arise from such superpositions are the origin of the characteristic fringes in the double-slit experiment and of the laser control scenarios. However, we have also shown that these two examples are fundamentally different: in the classical limit the interference contributions in the double-slit experiment are zero, while the interferences in laser control scenarios may survive and are the origins of classical laser control. What then is the difference between them? We provide several perspectives, below.

First, consider the issue from the viewpoint of the nature of the interference term. For example, consider the case of the excitation of a state of even parity to a given state in the continuum of energy $\mathscr{E}$ by a weak $\omega + 2\omega$ field of the form

$$E(t) = \epsilon_\omega \cos(\omega t + \phi_\omega) + \epsilon_{2\omega} \cos(2\omega t + \phi_{2\omega}). \tag{39}$$

The 2ω component is chosen to be exactly at resonance with the desired transition, and transfers population from the bound to the continuum state through one-photon absorption. In turn, the ω component couples bound and continuum states through a two-photon resonant excitation. Using second order perturbation theory we have that the field creates a superposition of the form:

$$|\psi\rangle = c_1|\mathscr{E}, \mathrm{odd}\rangle + c_2|\mathscr{E}, \mathrm{even}\rangle, \tag{40}$$

where the first term is due to the one-photon excitation by the 2ω field, and the second term is due to two-photon excitation by the ω field (a similar results holds even in the nonresonant case [27]). As a consequence note specifically that the coefficients c_1 and c_2 are proportional to $\epsilon_{2\omega}$ and ϵ_ω^2, respectively. The interference term, obtained from the cross product of the two terms, is then proportional to the amplitudes of the two fields as $\epsilon_{2\omega}\epsilon_\omega^2$. That is, the interference term is *driven* by the external field, a feature that is distinctly different from the traditional double-slit experiment where the interference term is field-free. It is this significant difference that manifests in the classical limit where the external driving field provides a classical contribution to the interference as well.

We emphasize that the interference term arising from Eq. (40), both quantum mechanically and in the classical limit, is then the collective effect of the two excitation routes. This is quite different from the double-slit experiment in the classical limit. Specifically, as long as the two slits are separated in space the quantum interference contributions will measure spatial coherences of the wavefunction that do not have a classical manifestation. This is so because classically passing through the upper or lower slit and arriving at the detection screen constitute two independent and mutually exclusive possibilities. By contrast, the response of a classical system to components of a radiation field do not constitute independent and mutually exclusive events.

These distinctions between the double-slit and the multiple-field induced dynamics are best seen in the response theory treatment [28] of the field induced dynamics. Consider again the case of excitation with an $\omega + 2\omega$ pulse. During the interaction of the system with a radiation field the photoinduced dipoles $\langle\mu\rangle$ are

$$\langle\mu\rangle = \chi^{(1)}E(t) + \chi^{(2)}E^2(t) + \chi^{(3)}E^3(t) + \cdots \tag{41}$$

Here, for simplicity, the response has been expressed in the adiabatic limit [28], where $\langle\mu\rangle$ depends only on the instantaneous values of the field amplitudes. Symmetry breaking in the response is characterized by terms in the polarization that survive time-averaging. The time-average of Eq. (41) is given by

$$\overline{\langle\mu\rangle} = \chi^{(1)}\overline{E(t)} + \chi^{(3)}\overline{E^3(t)} + \cdots, \tag{42}$$

where $\chi^{(2)} = 0$ for symmetric systems, and where the overbar denotes time-averaging. For $\omega + 2\omega$ fields, or any other AC field, $\overline{E(t)} = 0$, and the first term vanishes. However, the third-order term in the response is not necessarily zero. Rather, for the $\omega + 2\omega$ field in Eq. (39), it is given by

$$\overline{\langle\mu\rangle} = \chi^{(3)}\frac{3}{4}\epsilon_\omega^2\epsilon_{2\omega}\cos(2\phi_\omega - \phi_{2\omega}). \tag{43}$$

That is, the nonlinear response of the system to an $\omega + 2\omega$ field mixes the frequencies and harmonics of the incident radiation and leads to the generation of a phase-controllable zero-harmonic (dc) component in the response, i.e. the controlled symmetry breaking. This term arises because the net response of the system to the incident radiation is not just the sum of the responses to the individual components of the field [11]. The phenomenon requires a nonlinear response of the system to the laser field, and hence it applies to both quantum or classical systems with anharmonic potentials.

It is worth reemphazing that the matter interference effects and other entirely quantum contributions can have an important *quantitative* effect on the response [29,30]. However, the *qualitative* nonlinear response to the laser field that gives rise to laser controllable interference contributions does not necessarily rely upon them.

At this point the close connection between multiple-field induced based scenarios in Coherent Control and Nonlinear Optics is evident. Here, the crucial physics is the nonlinear response of matter to incident radiation. The difference between them relies on the focus. In Coherent Control the interest is on what happens with matter after the nonlinear interaction, whereas in Nonlinear Optics the concern is on what happens to the light after such an interaction.

One technical caveat is in order. The validity of the analysis in this paper relies on the correctness of the quantum-classical correspondence principle as developed in Section 3.1. It is through this principle that we are able to establish a connection between the quantum and classical subdivision of observables [Eqs. (15) and (35)], and to define classical analogs of quantum interference contributions. If this principle does not hold then it is possible that quantum and classical interference terms do not correspond to the same physical phenomenon. One case where this correspondence was clearly demonstrated to hold was our study of the $\omega + 2\omega$ control where the fields were incident on a quartic oscillator [11]. Specifically, we obtained an expression for the net dipole induced by $\omega + 2\omega$ fields in the Heisenberg picture and set $\hbar = 0$ to explicitly recover the classical limit of the interference contributions. In the quantum case, the net dipole induced by the field is of the form

$$\overline{\hat{x}^{\mathrm{H}}(t)} = \epsilon_\omega^2\epsilon_{2\omega}\hat{\Gamma}[\omega, \hbar, \hat{x}, \hat{p}]\cos(2\phi_\omega - \phi_{2\omega}), \tag{44}$$

where $\hat{\Gamma}[\omega, \hbar, \hat{x}, \hat{p}]$, the operator defining the quantum response, is a function of the laser frequency, the oscillator anharmonicity, and the position and momentum operators in Schrödinger picture. The classical solution extracted from the quantum solution is of the form:

$$\overline{x^c(t)} = \epsilon_\omega^2 \epsilon_{2\omega} \Gamma^c[\omega, x^c(0), p^c(0)] \cos(2\phi_\omega - \phi_{2\omega}), \quad (45)$$

where $\Gamma^c[\omega, x^c(0), p^c(0)]$ is the classical limit of $\hat{\Gamma}[\omega, \hbar, \hat{x}, \hat{p}]$, and $x^c(0)$ and $p^c(0)$ are the initial conditions for the classical position and momentum variables. A comparison of the classical behavior extracted in this way from the quantum solution with an independent fully classical calculation showed excellent agreement, explicitly demonstrating that the quantum and classical versions of laser control do qualitatively correspond to the same physical phenomenon. A couple of additional points are worth noting: (i) The structure of the Heisenberg result is a linear combination of classical and quantum contributions, with the latter vanishing in the classical limit. The quantum corrections arise due to the $\hbar$-dependence of the resonance structure of the oscillator. (ii) The cosine factor in Eqs. (44) and (45), showing the dependence of the symmetry breaking on the relative phase of the laser, does not contain an extra phase dependent on molecular properties (the molecular phase). This does not imply that the direction of the symmetry breaking can be predicted solely by looking at the form of the field since $\hat{\Gamma}[\omega, \hbar, \hat{x}, \hat{p}]$ and $\Gamma^c[\omega, x^c(0), p^c(0)]$ can be either positive or negative depending on the initial state and the laser frequency.

As for other control schemes, like 1 photon vs. 3 photons or bichromatic control – we would anticipate they and other schemes that rely on multiple interfering optically induced pathways to a have a qualitative classical limit, since these processes are common to both anharmonic classical and quantum systems [13,14]. For example, recent calculations [31] on the effect of an $\omega + 3\omega$ field (the field used in 1 vs. 3 control) on a classical Morse oscillator clearly show phase control on the photodissociation probability.

By contrast, other scenarios that are not based on the principle of interfering optically induced pathways may not have a classical manifestation. For example, the coherent control of bimolecular collisions at a fixed total energy, and for arbitrarily large collisional volumes, relies on creating entanglement between the internal and center of mass states [2] and, for this reason, is not expected to have a classical manifestation. However, recently proposed scenarios [32,33] that use nonentangled wave packets of translational motion to exert control of bimolecular collisions do have intuitive underlying classical pictures. Further studies are in order to ascertain when the classical limit, in cases where it exists, provides a quantitative approximation to the quantum control.

Acknowledgment

We thank NSERC for support of this research.

References

[1] M. Nielsen, I. Chuang, Quantum Computation and Quantum Information, Cambridge University Press, Cambridge, 2000.
[2] M. Shapiro, P. Brumer, Principles of the Quantum Control of Molecular Processes, John Wiley & Sons, New York, 2003.
[3] A. Daffertshofer, A.P.A. Plastino, Phys. Rev. Lett. 88 (2002) 210601.
[4] J. Wilkie, P. Brumer, Phys. Rev. A 55 (1997) 27.
[5] J. Wilkie, P. Brumer, Phys. Rev. A 55 (1997) 43.
[6] P. Brumer, J. Gong, Phys. Rev. A 73 (5) (2006) 052109.
[7] S.A. Rice, M. Zhao, Optical Control of Molecular Dynamics, John Wiley & Sons, New York, 2000.
[8] S.A. Rice, Nature 409 (2001) 422.
[9] H. Rabitz, R. de Vivie-Riedle, M. Motzkus, K. Kompa, Science 288 (2000) 824.
[10] T.A. Osborn, F.H. Molzahn, Ann. Phys. (NY) 241 (1995) 79.
[11] I. Franco, P. Brumer, Phys. Rev. Lett. 97 (2006) 040402.
[12] J. Pelc, J. Gong, P. Brumer, Phys. Rev. E 79 (6) (2009) 066207.
[13] P.W. Milloni, J.H. Eberly, Lasers, John Wiley & Sons, USA, 1988.
[14] R.W. Boyd, Nonlinear Optics, Academic Press, USA, 1992.
[15] H. Han, P. Brumer, J. Phys. B: Atomic Mol. Opt. Phys. 40 (9) (2007) S209.
[16] G. Greenstein, A.G. Zajonc, The Quantum Challenge: Modern Research on the Foundations of Quantum Mechanics, second ed., Jones and Bartlett, Sudbury, MA, 2006.
[17] M.P. Silverman, More than One Mystery, Springer-Verlag, New York, 1995.
[18] R.P. Feynman, R.B. Leighton, M. Sands, The Feynman Lectures on Physics, vol. 3, Addison-Wesley, Reading, MA, 1965.
[19] M. Arndt, O. Nairz, J. Vos-Andreae, C. Keller, G. van der Zouw, A. Zeilinger, Nature 401 (1999) 680.
[20] A.L. Fetter, J.D. Walecka, Quantum Theory of Many-Particle Systems, Dover, New York, 2003.
[21] M. Hillery, R.F. O'Connell, M.O. Scully, E.P. Wigner, Phys. Rep. 106 (1984) 121.
[22] V.I. Tatarskii, Sov. Phys. Usp. 26 (1983) 311.
[23] H.J. Groenewold, Physica 12 (1946) 405.
[24] T.A. Osborn, M.F. Kondratieva, J. Phys. A: Math. Gen. 35 (2002) 5279.
[25] I. Franco, P. Brumer, J. Phys. B: Atomic Mol. Opt. Phys. 41 (7) (2008) 074003.
[26] M. Spanner, I. Franco, P. Brumer, Phys. Rev. A 80 (2009) 053402.
[27] I. Franco, Coherent control of laser-induced symmetry breaking: from fundamentals to applications, Ph.D. Thesis, University of Toronto, 2007.
[28] P.N. Butcher, D. Cotter, The Elements of Nonlinear Optics, Cambridge University Press, New York, 1990.
[29] M. Kryvohuz, J. Cao, Phys. Rev. Lett. 96 (2006) 030403.
[30] M. Kryvohuz, R. Loring, J. Chem. Phys. 128 (2008) 124106.
[31] V. Constantoudis, C.A. Nicolaides, J. Chem. Phys. 122 (2005) 084118.
[32] M. Spanner, P. Brumer, Phys. Rev. A 76 (2007) 013408.
[33] M. Spanner, P. Brumer, Phys. Rev. A 76 (2007) 013409.